Pragya Sharma,[1] Edward B. Arias,[1] and Gregory D. Cartee[1,2,3]

Protein Phosphatase 1-α Regulates AS160 Ser^{588} and Thr^{642} Dephosphorylation in Skeletal Muscle

Diabetes 2016;65:2606–2617 | DOI: 10.2337/db15-0867

SIGNAL TRANSDUCTION

Akt substrate of 160 kDa (AS160) phosphorylation on Thr^{642} and Ser^{588} by Akt is essential for insulin's full effect on glucose transport. However, protein phosphorylation is determined by the balance of actions by kinases and phosphatases, and the specific phosphatase(s) controlling AS160 dephosphorylation is (are) unknown. Accordingly, we assessed roles of highly expressed skeletal muscle serine/threonine phosphatases (PP1, PP2A, PP2B, and PP2C) on AS160 dephosphorylation. Preliminary screening of candidate phosphatases used an AS160 dephosphorylation assay. Lysates from insulin-stimulated skeletal muscle were treated with pharmacological phosphatase inhibitors and assessed for AS160 Ser^{588} and Thr^{642} dephosphorylation. AS160 dephosphorylation on both phosphorylation sites was unaltered by PP2B or PP2C inhibitors. Okadaic acid (low dose inhibits PP2A; high dose inhibits PP1) delayed AS160 Ser^{588} (both doses) and Thr^{642} (high dose only) dephosphorylation concomitant with greater Akt phosphorylation (both doses). AS160 was coimmunoprecipitated with PP1-α but not with PP1-β, PP1-γ1, or PP2A. Recombinant inhibitor-2 protein (a selective PP1 inhibitor) delayed AS160 dephosphorylation on both phosphorylation sites without altering Akt phosphorylation. Furthermore, knockdown of PP1-α but not PP1-β or PP1-γ1 by small interfering RNA caused greater AS160 Ser^{588} and Thr^{642} phosphorylation concomitant with unaltered Akt phosphorylation. Together, these results identified PP1-α as a regulator of AS160 Thr^{642} and Ser^{588} dephosphorylation in skeletal muscle.

Skeletal muscle accounts for the largest portion of insulin-mediated whole-body glucose disposal, and skeletal muscle insulin resistance is crucial for whole-body insulin resistance and type 2 diabetes (1). Muscle insulin resistance is secondary, in large part, to defective GLUT4 translocation and glucose transport (2). Insulin's stimulation of glucose transport is triggered by a complex insulin-signaling pathway that begins with insulin's binding to its receptor, leading to receptor autophosphorylation and activation of receptor tyrosine kinase (2). The insulin receptor kinase phosphorylates insulin receptor substrate (IRS) proteins on multiple tyrosine residues, resulting in IRS protein engagement with phosphatidylinositol (PI) 3-kinase (PI3K), that in turn, phosphorylates PI 4,5-bisphosphate to create 3,4,5-trisphosphate (PIP3). The serine/threonine kinase Akt is recruited to bind PIP3 and become activated secondary to phosphorylation on Thr^{308} via phosphoinositide-dependent kinase-1 (PDK1) and Ser^{473} via mTORC2. Akt phosphorylates many protein substrates, several of which have been implicated in insulin's regulation of GLUT4 traffic to the cell surface membranes, including a Rab-GTPase activating protein known as Akt substrate of 160 kDa (AS160; also known as TBC1D4) (3–5). Akt can phosphorylate several residues on AS160. Mutation of serine or threonine to alanine to prevent phosphorylation of Ser^{588} or Thr^{642} resulted in attenuation of insulin-stimulated GLUT4 translocation, and mutation of several other Akt phosphomotifs did not produce any further effects on GLUT4 localization (6). Fully understanding the regulation of AS160 phosphorylation is essential given the crucial role that it plays in regulating insulin-stimulated glucose uptake by skeletal muscle.

The reversible serine/threonine phosphorylation of proteins is balanced by the opposing actions of kinases and

[1]Muscle Biology Laboratory, School of Kinesiology, University of Michigan, Ann Arbor, MI
[2]Department of Molecular and Integrative Physiology, University of Michigan, Ann Arbor, MI
[3]Institute of Gerontology, University of Michigan, Ann Arbor, MI
Corresponding author: Gregory D. Cartee, gcartee@umich.edu.

Received 24 June 2015 and accepted 23 May 2016.

phosphatases, but for most proteins, there has been an overwhelming bias to focus on serine/threonine kinases, with strikingly fewer studies assessing the role of serine/threonine phosphatases (7). Serine/threonine protein phosphatases regulate diverse aspects of growth, development, and metabolism, but relatively few protein serine/threonine phosphatases control the specific dephosphorylation of a much greater number of phosphoprotein substrates (8). With specific regard to AS160, many studies have analyzed the role of Akt in the insulin-stimulated phosphorylation of AS160 (9–13), but essentially nothing is known about the serine/threonine protein phosphatase(s) regulating AS160 dephosphorylation.

Protein phosphatase 1 (PP1), PP2A, PP2B, and PP2C are among the most abundant serine/threonine protein phosphatases expressed by skeletal muscle (14), and we hypothesized that AS160 dephosphorylation on Thr^{642} and Ser^{588} would be regulated by one or more of these enzymes. We evaluated the hypothesis using multiple approaches, including assessment of

1. the effects of several pharmacologic serine/threonine protein phosphatase inhibitors on AS160 Ser^{588} and Thr^{642} dephosphorylation;
2. the physical association of AS160 with serine/threonine protein phosphatases;
3. the influence of a selective inhibitor of PP1, known as inhibitor 2 (Inh-2) (15), on AS160 Ser^{588} and Thr^{642} phosphorylation; and
4. the consequences of knockdown of serine/threonine protein phosphatases by small interfering (si)RNA silencing on AS160 Ser^{588} and Thr^{642} phosphorylation.

These experiments identified PP1-α as a serine/threonine protein phosphatase that regulates AS160 Ser^{588} and Thr^{642} dephosphorylation in skeletal muscle.

RESEARCH DESIGN AND METHODS

Materials

The reagents and apparatus for SDS-PAGE and nonfat dry milk (#170-6404XTU) were from Bio-Rad (Hercules, CA). MemCode Reversible Protein Stain (#24580) and bicinchoninic acid (#23227) protein assay kits and tissue protein extraction reagent (T-PER; #78510) were from Thermo Fisher (Waltham, MA). Luminata Forte Western HRP Substrate (#WBLUF0100) was from EMD Millipore (Billerica, MA). Sanguinarine chloride (#ALX-350-076) was from Enzo Life Sciences (Farmingdale, NY). FK-506 (#3631) was purchased from Tocris (Bristol, U.K.). Okadaic acid (OA; #459620) was purchased from Merck Millipore (Billerica, MA). Recombinant protein phosphatase Inh-2 (#P0755) was from New England Biolabs (Ipswich, MA). Anti-phosphorylated (p)Akt^{Thr308} (#9275), anti-$pAkt^{Ser473}$ (#9271), anti-Akt (#4691), anti-$pAS160^{Thr642}$ (#8881), anti-$pAS160^{Ser588}$ (#8730), anti–PP1-α (#2582), anti-spinophilin (#14136), and anti-rabbit IgG horseradish peroxidase conjugate (#7074) were from Cell Signaling Technology (Danvers, MA). Anti-AS160 (#ABS54), anti–PP1-β (#07–1217), anti–PP1-γ1 (#07-1218), anti–α-tubulin (#04-1117), and normal rabbit IgG polyclonal antibody control (#12-370) were purchased from EMD Millipore. Anti-PP2Aα (#610556) was from BD Bioscience (San Jose, CA). PP1 Inh-2 antibody (#AF4719) was from R&D Biosystems (Minneapolis, MN). Anti–PP1-α (#sc-443), anti-GADD34 (#sc-8327), anti-goat IgG horseradish peroxidase conjugate (#sc-2020), and anti-mouse IgG horseradish peroxidase conjugate (#sc-2060), were from Santa Cruz Biotechnology (Santa Cruz, CA). Anti-phostensin (#MB1057) was from BioWorld Technology, Inc. (St. Louis Park, MN). siRNA against rat PP1 catalytic subunits α (#L-100270-02-0020), β (#L-100263-02-0020), or γ1 (#L-096319-02-0020) and RNA interference-negative control (#D-001810-10-20) were purchased as SMARTpools from Dharmacon (Lafayette, CO). Protein G magnetic beads (#10004D), RNAiMAX transfection reagent (#13778-150), and DMEM (#11995) were from Life Technologies (Grand Island, NY).

Animal Treatment

Procedures for animal care were approved by the University of Michigan Committee on Use and Care of Animals. Male Wistar rats (aged 8–10 weeks) were from Harlan (Indianapolis, IN). Lean (*Fa/Fa*) and obese (*fa/fa*) male Zucker rats (aged 7–8 weeks) were from Charles River Laboratories (Wilmington, MA). Animals were provided with rodent chow (Lab Diet No. 5001; PMI Nutrition International, Brentwood, MO) ad libitum until 1700 h the night before the experiment, when food was removed. The next day at 1000 h to 1200 h, rats were anesthetized (intraperitoneal injection of sodium pentobarbital), and both epitrochlearis muscles were isolated and treated as described below.

Muscle Incubation

Isolated epitrochlearis muscles were incubated in glass vials containing Krebs-Henseleit buffer, 0.1% BSA, 2 mmol/L sodium pyruvate, 6 mmol/L mannitol, without (basal) or with insulin at 0.6 nmol/L (for coimmunoprecipitation [Co-IP] assays described below) or 30 nmol/L (for dephosphorylation assays described below) for 30 min in a heated, shaking water bath at 35°C with continuous gassing (95% O_2 and 5% CO_2). Immediately after the incubation, muscles were blotted, rapidly trimmed of connective tissue, and freeze-clamped with liquid N_2–cooled aluminum tongs. Frozen muscles were stored at −80°C until subsequent homogenization and analysis.

L6 Cell Culture and Treatment

L6 myoblasts were purchased from the American Type Culture Collection (Manassas, VA). L6 cells were cultured in DMEM, supplemented with 10% (vol/vol) FBS, 1% penicillin, and 100 μg/mL streptomycin in a humidified atmosphere with 5% CO_2 at 37°C. Cells were washed twice with 1× PBS, and starved for 5 h in serum-free DMEM medium before 20 min of incubation without insulin (basal) or with insulin (100 nmol/L).

Muscle and Cell Lysate Preparation

Unless otherwise noted, epitrochlearis muscles were homogenized (TissueLyser II homogenizer; Qiagen Inc., Valencia, CA) using ice-cold T-PER buffer supplemented with 2.5 mmol/L sodium pyrophosphate, 1 mmol/L sodium vanadate, 1 mmol/L β-glycerophosphate, 1 μg/mL leupeptin, 1 μg/mL pepstatin, 1 μg/mL aprotinin, and 1 mmol/L phenylmethyl sulfonyl fluoride (PMSF). Homogenates were then transferred to microcentrifuge tubes and rotated (1 h, 4°C) before being centrifuged (15,000*g*, 20 min, 4°C). L6 cells were scraped in T-PER that was supplemented as described above, incubated (4°C, 20 min), and then centrifuged (15,000*g*, 20 min, 4°C). Total protein in supernatants from muscle or cell lysates was measured by the bicinchoninic acid method.

Epitrochlearis muscles and L6 cells used for Co-IP were processed as described above using Co-IP buffer (50 mmol/L HEPES [pH 7.5], 150 mmol/L NaCl, 1% IGEPAL, 10% glycerol) supplemented with 2.5 mmol/L sodium pyrophosphate, 1 mmol/L sodium vanadate, 1 mmol/L β-glycerophosphate, 1 μg/mL leupeptin, 1 μg/mL pepstatin, 1 μg/mL aprotinin, and 1 mmol/L PMSF.

Epitrochlearis muscles used for the dephosphorylation assay described below were homogenized for 2 min in cold T-PER buffer supplemented with 1 μg/mL leupeptin, 1 μg/mL pepstatin, 1 μg/mL aprotinin, and 1 mmol/L PMSF, but without phosphatase inhibitors (2.5 mmol/L sodium pyrophosphate, 1 mmol/L sodium vanadate, 1 mmol/L β-glycerophosphate). Lysates were centrifuged (15,000*g*, 2 min, 4°C), and the resultant supernatants were immediately used for the dephosphorylation assay described below.

AS160 Dephosphorylation Assay

Preliminary insights about the regulation of AS160 dephosphorylation were provided by testing the ability of several chemical phosphatase inhibitors, with differing specificity for inhibiting selected protein phosphatases, to delay the rate of AS160 dephosphorylation in lysates prepared from isolated epitrochlearis muscles. The AS160 dephosphorylation assay was a modification of a method previously used to identify the serine/threonine phosphatase that dephosphorylates calcium-binding protein 4 (16) The muscles used for this AS160 dephosphorylation assay were first incubated with 30 nmol/L insulin to ensure initially high levels of AS160 phosphorylation. Freeze-clamped muscles were rapidly homogenized in ice-cold buffer in the absence of protein phosphatase inhibitors. An initial aliquot (20 μL) was rapidly withdrawn from each muscle lysate and immediately mixed with an equal volume of 2× SDS loading buffer and heated (95°C, 6 min). This initial aliquot was denoted as the 0-min time point for the AS160 dephosphorylation assay. To the remaining lysate, a chemical protein phosphatase inhibitor (5 nmol/L OA for PP2A inhibition and 1,000 nmol/L OA for PP1 inhibition (17); 10 μmol/L sanguinarine for PP2C inhibition (18); or 100 ng/mL FK-506 for PP2B inhibition (19)) or an equal volume of vehicle (DMSO) was rapidly added. The lysates were then incubated at 37°C, with aliquots (20 μL) withdrawn at 30, 60, and 120 min. Upon withdrawal, each aliquot was rapidly mixed with an equal volume of 2× SDS loading buffer and heated to 95°C for 6 min. SDS-PAGE and immunoblotting were used to assess the phosphorylation levels of $AS160^{Ser588}$ and $AS160^{Thr642}$ in these aliquots. When Inh-2 protein was used, dephosphorylation assays were performed as described above for chemical inhibitors, except that epitrochlearis lysates were incubated with or without recombinant Inh-2 (rInh-2) protein (50 μg/mL lysate) rather than a chemical inhibitor. Dephosphorylation assays in lean Zucker (LZ) and obese Zucker (OZ) rats were performed as described above, except lysates were incubated without any phosphatase inhibitors.

Co-IP

IP was performed in lysates prepared from epitrochlearis muscles (300 μg total protein) and L6 cells (400 μg total protein) using AS160 antibody or normal rabbit IgG at 4°C overnight. The next morning, the protein-antibody complex was incubated with 50 μL magnetic protein G beads for 2 h at 4°C with gentle rotation. The antibody-protein-beads complex was washed three times with Co-IP buffer. The protein in the complex was then eluted with 30 μL of 2× SDS loading buffer and boiled before running on a polyacrylamide gel. Proteins were transferred to polyvinylidene fluoride membranes, and AS160-associated proteins were immunoblotted using antibodies against PP1-α, PP1-β, PP1-γ1, and PP2A. The association of AS160 with PP1-α was also assessed by IP using anti–PP1-α, followed by immunoblotting with anti-AS160. In addition, the association of AS160 with several PP1-α regulatory subunits (20–22) was evaluated by immunoprecipitation using anti-AS160, followed by immunoblotting with antibodies against spinophilin (also known as PPP1R9B), GADD34 (also known as PPP1R15A), phostensin (also known as PPP1R18), and Inh-2 (also known as PPP1R2).

siRNA Silencing

L6 cells were transfected with 200 nmol/L control scrambled siRNA, siPP1-α, siPP1-β, or siPP1-γ1 using RNAiMAX transfection reagent from Invitrogen using the manufacturer's instructions, with minor modifications. Briefly, cells were seeded in 60-mm plates at 50% confluence in DMEM supplemented with 10% FBS. On day 2, myoblasts were transfected with 200 nmol/L of siRNA in reduced serum Opti-MEM media without antibiotics. The media changed 48 h later to DMEM supplemented with 10% FBS. At 72 h of transfection, the cells were treated without insulin (basal) or with 100 nmol/L insulin in serum-free medium for 20 min before being harvested. The extent of PP1-α, PP1-β, or PP1-γ1 knockdown was assessed by immunoblot.

Immunoblotting

Equal amounts of protein from each sample were loaded on a Tris glycine acrylamide gel and transferred to polyvinylidene fluoride membrane. The membranes were incubated

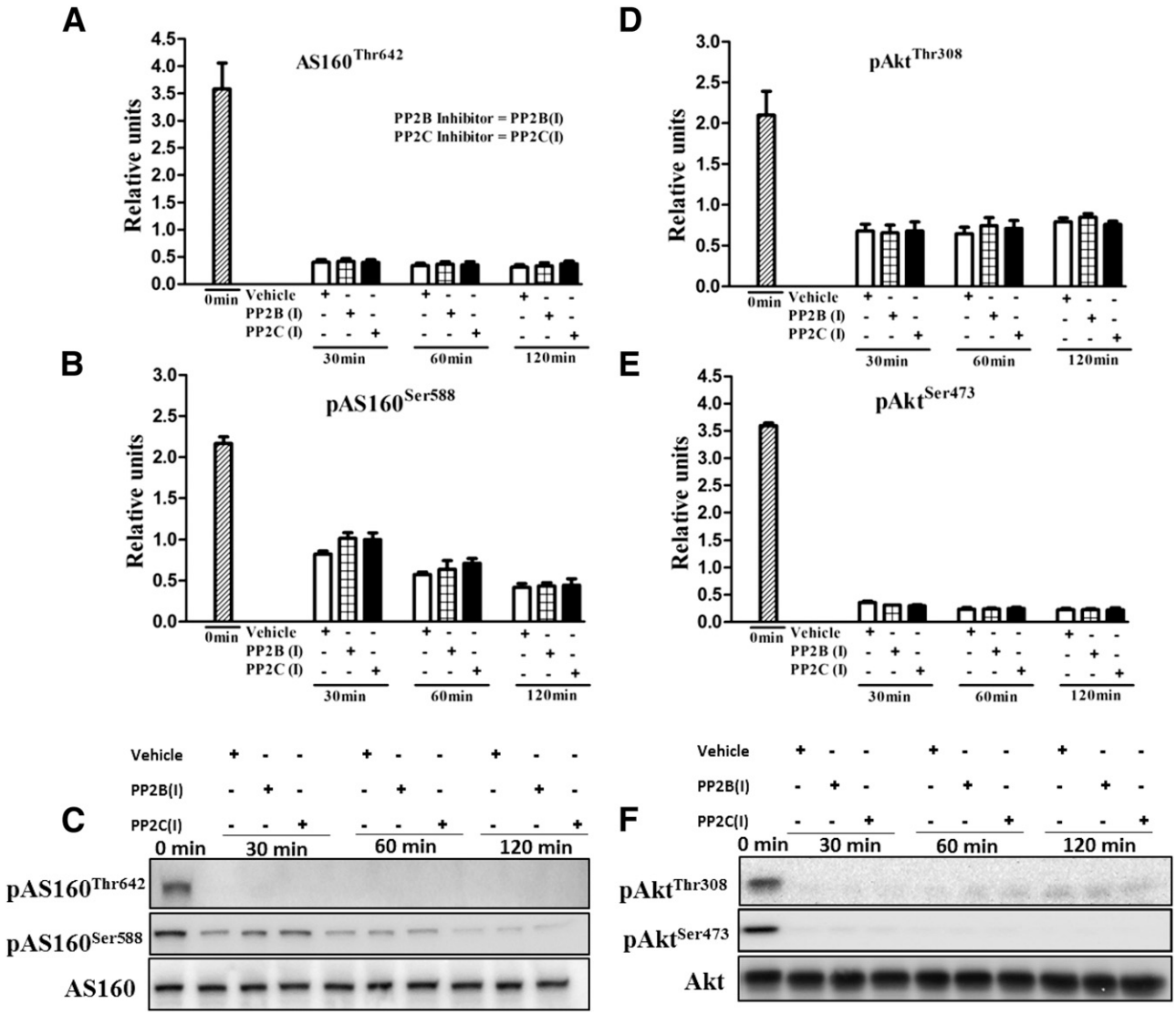

Figure 1—Effects of the PP2B inhibitor FK-506 (100 ng/mL) and the PP2C inhibitor sanguinarine (10 μmol/L) on AS160 phosphorylation in epitrochlearis muscles. The time course for AS160 dephosphorylation was assessed using isolated muscles that were incubated with insulin (30 nmol/L) before being rapidly homogenized. To determine initial AS160 phosphorylation, an aliquot from each lysate was immediately combined with 2× SDS buffer to stop dephosphorylation (denoted as 0 min). Aliquots from the remaining lysate were incubated for 30, 60, or 120 min at 37°C in the presence of vehicle, FK-506, denoted as PP2B (I), or the sanguinarine, denoted as PP2C (I). After each incubation time, lysates were combined with 2× SDS buffer before undergoing immunoblotting: pAS160^{Thr642} (*A*); AS160^{Ser588} (*B*); representative immunoblots of pAS160^{Thr642}, pAS160^{Ser588}, and total AS160 (*C*); pAkt^{Thr308} (*D*); pAkt^{Ser473} (*E*); and representative immunoblots of pAkt^{Thr308}, pAkt^{Ser473}, and total Akt (*F*). Values are expressed as mean ± SEM (n = 4 muscle lysates per treatment). Data were analyzed using one-way ANOVA.

with appropriate primary and secondary antibodies. Immunoreactive proteins were detected using Luminata Forte Western HRP Substrate and quantified by densitometry (Alpha Innotech, San Leandro, CA).

Statistical Analysis

Statistical analyses were performed using Prism 4.0 software (GraphPad Software, La Jolla, CA). Data are expressed as means ± SEM. Differences between two groups were evaluated using a two-tailed t test. Differences between more than two groups were evaluated using one-way ANOVA. The source of significant variance was identified using Tukey post hoc analysis. A P value of ≤ 0.05 was considered statistically significant.

RESULTS

Neither FK-506 nor Sanguinarine Delay AS160 Dephosphorylation

Neither the PP2B inhibitor FK-506 nor the PP2C inhibitor sanguinarine differed from the vehicle for pAS160^{Thr642} (Fig. 1*A* and *C*) or pAS160^{Ser588} (Fig. 1*B* and *C*) in epitrochlearis muscle lysates. Similarly, neither inhibitor differed from vehicle for pAkt^{Thr308} (Fig. 1*D* and *F*) or pAkt^{Ser473} (Fig. 1*E* and *F*). These results

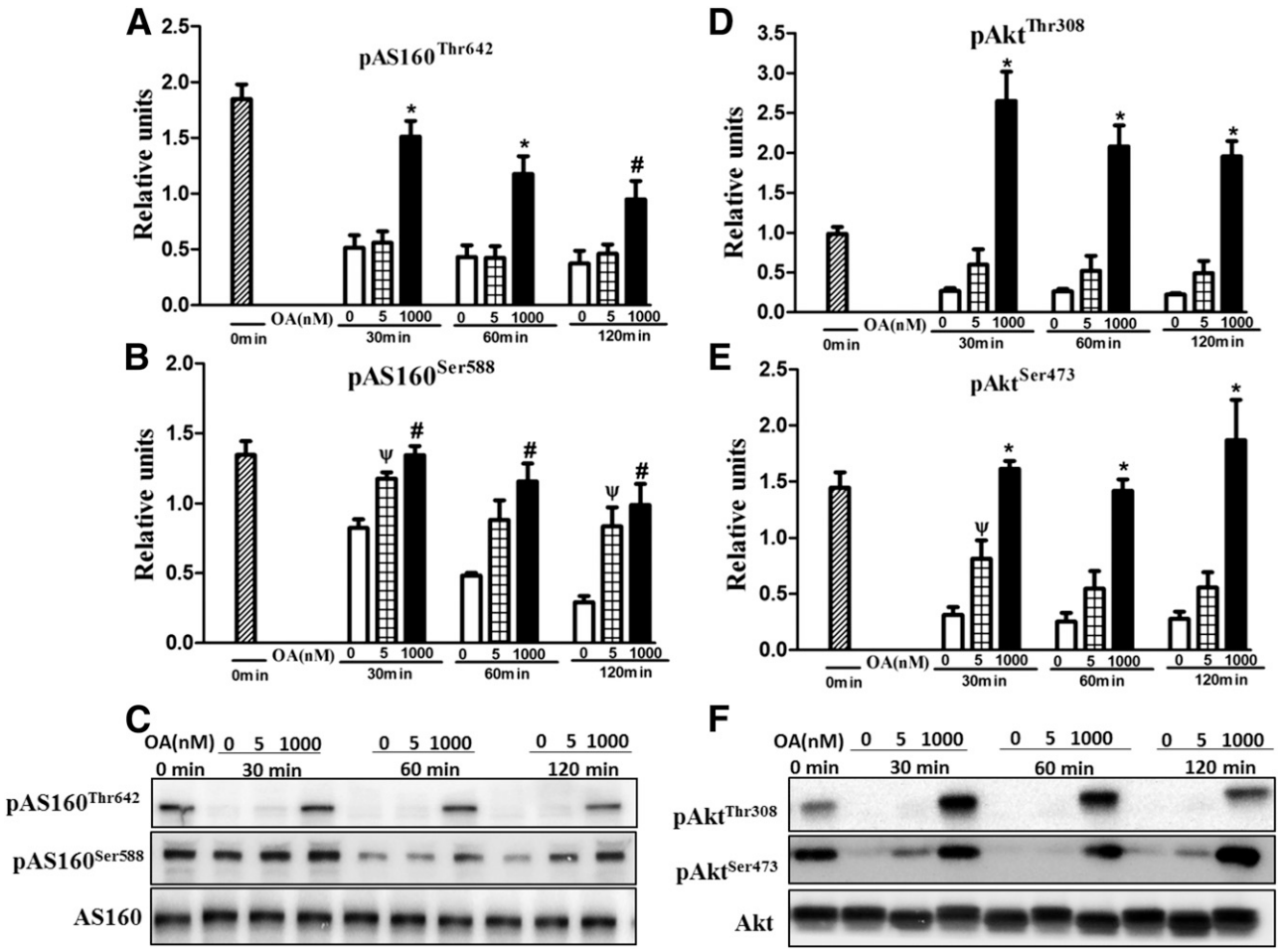

Figure 2—Effects of OA (5 nmol/L for PP2A inhibition or 1,000 nmol/L for PP1 inhibition) on AS160 dephosphorylation in epitrochlearis muscles. The procedure described for Fig. 1 was used except that OA was the phosphatase inhibitor used rather than FK-506 or sanguinarine: pAS160^{Thr642} (*A*); AS160^{Ser588} (*B*); representative immunoblots of pAS160^{Thr642}, pAS160^{Ser588}, and total AS160 (*C*); pAkt^{Thr308} (*D*); pAkt^{Ser473} (*E*); and representative immunoblots of pAkt^{Thr308}, pAkt^{Ser473}, and total Akt (*F*). Values are expressed as mean ± SEM (n = 4 muscle lysates per treatment). Data were analyzed using one-way ANOVA. Tukey post hoc analysis was performed to identify the source of significant variance. *P < 0.05, 1,000 nmol/L OA exceeds both 0 and 5 nmol/L OA at the corresponding time; #P < 0.05, 1,000 nmol/L OA exceeds 0 nmol/L OA at the corresponding time; ψP < 0.05, 5 nmol/L exceeds 0 nmol/L OA at the corresponding time.

provide no evidence that PP2B or PP2C regulate AS160 dephosphorylation.

Dose-Dependent Effects of OA on AS160 Dephosphorylation

There were no differences for the phosphorylation of AS160^{Thr642} of epitrochlearis muscle lysates treated with vehicle compared with 5 nmol/L OA, a dose sufficient to inhibit PP2A but not PP1 (23) at 30, 60, and 120 min. In contrast, for lysates treated with 1,000 nmol/L OA, a dose sufficient to inhibit PP1 (23), the phosphorylation of AS160^{Thr642} was significantly ($P < 0.05$) greater than the vehicle at 30, 60, and 120 min and significantly ($P < 0.05$) greater than the 5 nmol/L OA values at 30 and 60 min (Fig. 2*A* and *C*). For phosphorylation of AS160^{Ser588}, the values with 5 nmol/L OA significantly ($P < 0.05$) exceeded the vehicle at 30 and 120 min, and the 1,000 nmol/L values were significantly ($P < 0.05$) greater than vehicle at 30, 60, and 120 min (Fig. 2*B* and *C*). For phosphorylation of Akt^{Thr308}, there were no significant differences between the 5 nmol/L OA values and vehicle at 30, 60, and 120 min, but the 1,000 nmol/L values significantly ($P < 0.05$) exceeded both vehicle and 5 nmol/L OA values at 30, 60, and 120 min (Fig. 2*D* and *F*). For phosphorylation of Akt^{Ser473}, the values with 5 nmol/L OA were significantly ($P < 0.05$) greater than vehicle at 30 min, and the 1,000 nmol/L OA values significantly ($P < 0.05$) exceeded vehicle and 5 nmol/L values at 30, 60, and 120 min (Fig. 2*E* and *F*). Taken together, these results suggest that AS160 dephosphorylation is influenced by OA in a dose-dependent and site-selective manner. Only the higher OA dose delayed dephosphorylation of AS160^{Thr642}, which would be consistent with an effect related to inhibition of PP1. In

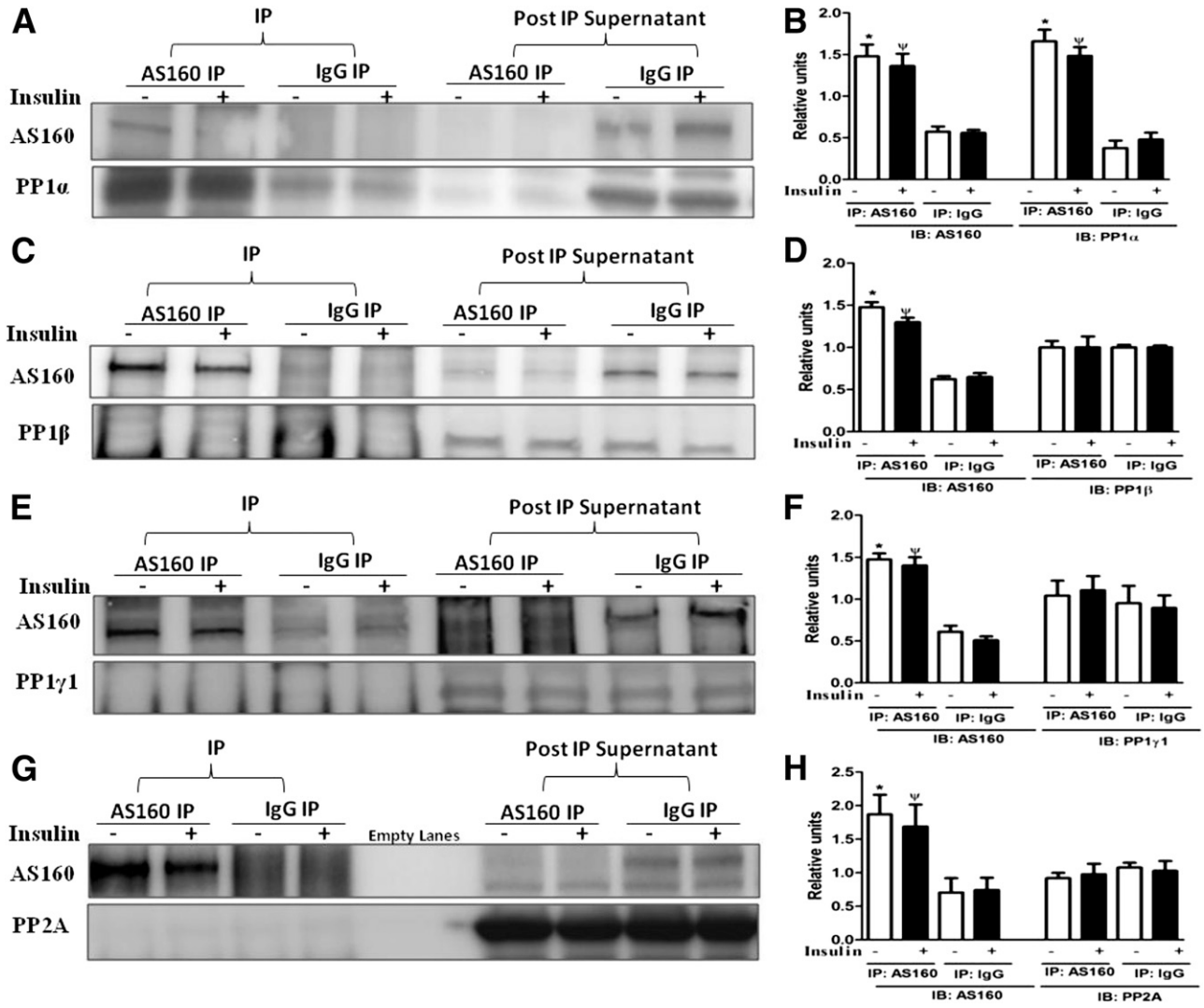

Figure 3—Co-IP of PP1-α, PP1-β, PP1-γ1, and PP2A with AS160 in epitrochlearis muscles. Anti-AS160 antibody was used to precipitate AS160 in lysates prepared from isolated muscles that had been incubated with or without insulin, and IgG was used as a control for nonspecific Co-IP. Immune complexes were immunoblotted for AS160, PP1-α, PP1-β, PP1-γ1, and PP2A. Representative immunoblots (IBs) (*A*) and data (*B*) for the Co-IP of PP1-α with AS160. Representative IBs (*C*) and data (*D*) for the Co-IP of PP1-β with AS160. Representative IBs (*E*) and data (*F*) for the Co-IP of PP1-γ1 with AS160. Representative IBs (*G*) and data (*H*) for the Co-IP of PP2A with AS160. Values are expressed as mean ± SEM (n = 3–4 per treatment). Data were analyzed using a two-tailed t test. *$P < 0.05$, IP using anti-AS160 exceeds IP using IgG control for lysates from muscles incubated without insulin; ψ$P < 0.05$, IP using anti-AS160 exceeds IP using IgG control for lysates from muscles incubated with insulin.

contrast, both OA doses delayed dephosphorylation of $AS160^{Ser588}$, suggesting possible roles of PP2A and/or PP1.

Selective AS160 Co-IP With PP1-α but Not PP1-β, PP1-γ1, or PP2A

Because the OA results were not definitive, we used additional approaches to probe the relationship of AS160 with PP1 and PP2A in skeletal muscle. Specific interaction between PP1-α and AS160 in epitrochlearis was indicated by the significantly ($P < 0.05$) greater amount of PP1-α that Co-IP with AS160 compared with normal IgG control regardless of insulin concentration (Fig. 3*A* and *B*). The specific association between AS160 and PP1-α was confirmed by IP using anti–PP1-α, followed by immunoblotting with anti-AS160, compared with normal IgG control (data not shown). In contrast, there was no evidence that AS160 had any specific association with PP-β1 (Fig. 3*C* and *D*), PP1-γ1 (Fig. 3*E* and *F*), or PP2A (Fig. 3*G* and *H*). Similar results were obtained for L6 cells in which specific interaction was detected for AS160 with PP1-α but not for AS160 with PP1-β, PP1-γ1, or PP2A (data not shown). The selective association of AS160 with PP1-α supports the idea that PP1-α may regulate AS160 dephosphorylation. The association of AS160 with several PP1-α regulatory subunits (spinophilin, GADD34, phostensin, and Inh-2) was evaluated in epitrochlearis lysates immunoprecipitated

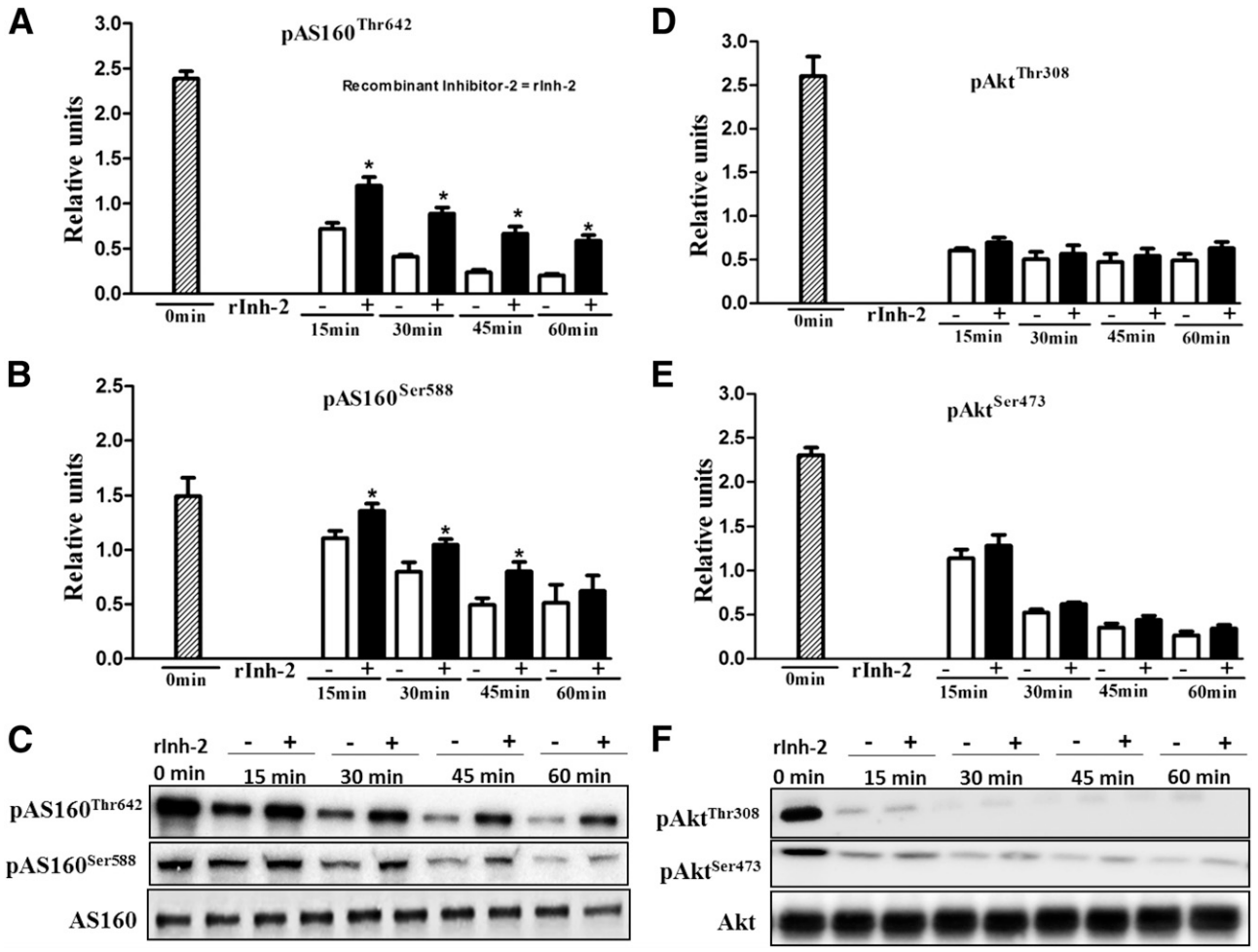

Figure 4—Effects of rInh-2 on AS160 dephosphorylation in epitrochlearis muscles. The procedure described for Fig. 1 was used except that the specific PP1 inhibitor protein rInh-2 was assessed rather than pharmacologic inhibitors: pAS160^{Thr642} (*A*); AS160^{Ser588} (*B*); representative immunoblots of pAS160^{Thr642}, pAS160^{Ser588}, and total AS160 (*C*); pAkt^{Thr308} (*D*); pAkt^{Ser473} (*E*); and representative immunoblots of pAkt^{Thr308}, pAkt^{Ser473}, and total Akt (*F*). Values are expressed as mean ± SEM (n = 4 muscle lysates per treatment). Data were analyzed using a two-tailed t test. *$P < 0.05$, plus rInh-2 exceeds minus rInh-2.

using anti-AS160, followed by immunoblotting with antibodies against the respective regulatory subunits. However, this analysis did not detect evidence of selective association of these proteins with AS160 (data not shown).

rInh-2 Protein Delays AS160 Dephosphorylation

Inh-2 was studied because it is a selective biological inhibitor of PP1 (15). Epitrochlearis lysates incubated with rInh-2 protein compared with control lysates had greater ($P < 0.05$) phosphorylation of AS160^{Thr642,} at 15, 30, 45, and 60 min (Fig. 4*A* and *C*). Furthermore, rInh-2 treatment versus controls produced greater ($P < 0.05$) phosphorylation of AS160^{Ser588} at 15, 30, and 45 min (Fig. 4*B* and *C*). Greater AS160 phosphorylation was not accompanied by any significant effects of rInh-2 on the phosphorylation of Akt^{Thr308} (Fig. 4*D* and *F*) or Akt^{Ser473} (Fig. 4*E* and *F*). The delayed AS160 dephosphorylation on both Thr^{642} and Ser^{588} with unaltered Akt phosphorylation is consistent with PP1 being a modulator of AS160 dephosphorylation.

Silencing PP1-α but Not Other PP1 Isoforms Leads to Greater AS160 Phosphorylation

Because PP1-α was selectively associated with AS160 based on Co-IP, it was also critical to perform a functional assessment of the roles of PP1 isoforms on AS160's phosphorylation status in intact muscle cells. L6 cells transfected with siPP1-α had a significant ($P < 0.05$) reduction in PP1-α protein abundance compared with cells transfected with scrambled control siRNA (Fig. 5*A*). The specificity of the PP1-α knockdown in the siPP1-α–transfected cells was evidenced by the lack of changes in PP1-β or PP1-γ1 protein levels (Fig. 5*B*). Lower PP1-α abundance led to significantly ($P < 0.05$) greater phosphorylation of AS160^{Thr642} (Fig. 5*C*) and AS160^{Ser588} (Fig. 5*D*) in the insulin-stimulated siPP1-α–transfected cells compared with insulin-stimulated control

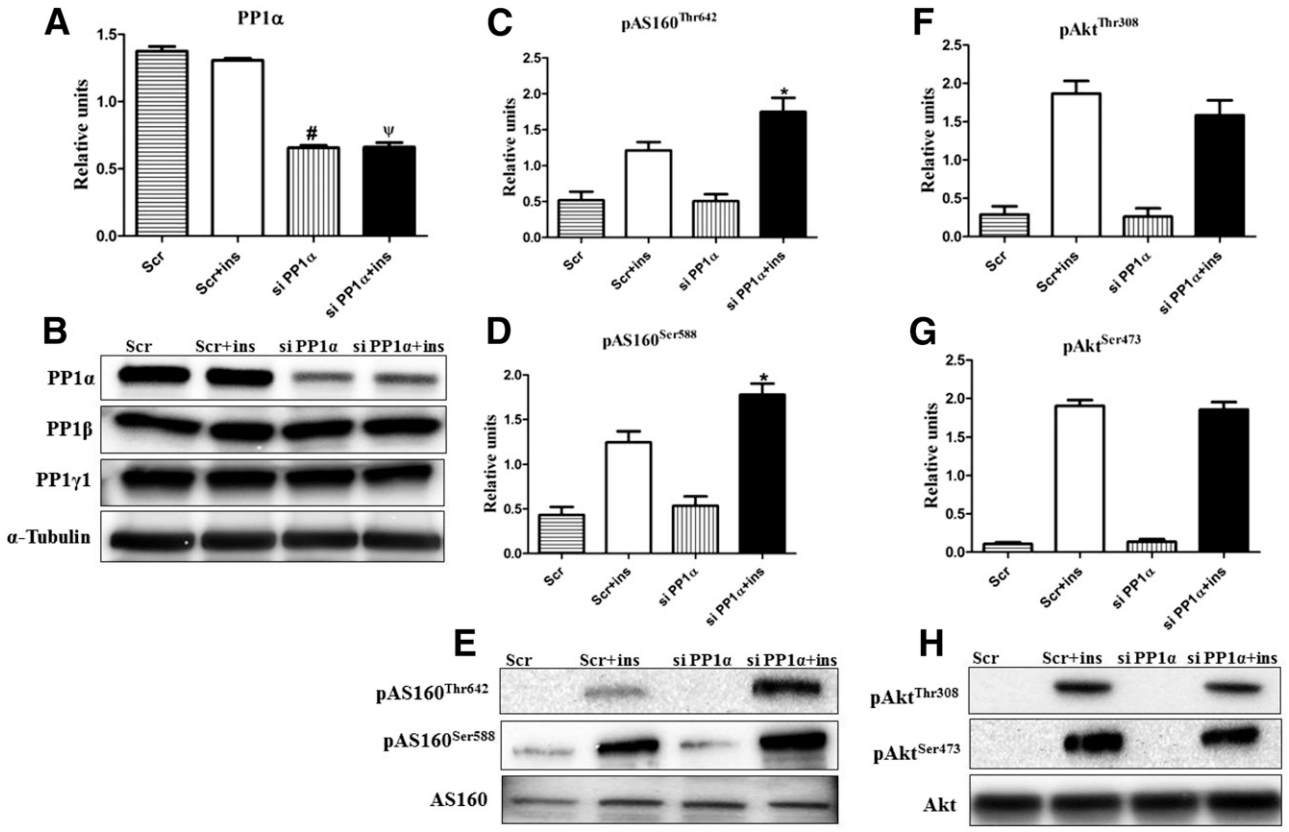

Figure 5— Effects of silencing the PP1-α on AS160 phosphorylation in L6 myocytes. Cells were transfected with siPP1-α or scrambled (Scr) siRNA. At 72 h after transfection, cells were incubated without or with insulin (ins; 100 nmol/L) for 20 min. Protein abundance and phosphorylation were assessed by immunoblotting. PP1-α (A); representative immunoblots of PP1-α, PP1-β, PP1-γ1, and α-tubulin (*B*); pAS160^{Thr642} (*C*); pAS160^{Ser588} (*D*); representative immunoblots of AS160^{Thr642}, pAS160^{Ser588}, and AS160 (*E*); pAkt^{Thr308} (*F*); pAkt^{Ser473} (*G*); and representative immunoblots of pAkt^{Thr308}, pAkt^{Ser473}, and Akt (*H*). Values are expressed as mean ± SEM (n = 5–6 experiments). Data were analyzed using a two-tailed t test. #$P < 0.05$, siPP1-α is less than Scr for cells incubated without insulin. ψ$P < 0.05$, siPP1-α is less than Scr for cells incubated with insulin. *$P < 0.05$, siPP1-α exceeds Scr for cells incubated with insulin.

cells. Greater AS160 phosphorylation was not attributable to any effect of siPP1-α transfection on the phosphorylation of Akt^{Thr308} (Fig. 5*F*) or Akt^{Ser473} (Fig. 5*G*).

Transfection of L6 cells with siPP1-β produced a robust and significant ($P < 0.05$) reduction in PP1-β protein abundance compared with cells transfected with scrambled control siRNA (Fig. 6*A*). The specificity of the PP1-β knockdown was confirmed by the absence of changes in PP1-α or PP1-γ1 abundance (Fig. 6*B*). The lower PP1-β content had no detectable effects on the phosphorylation of AS160^{Thr642} (Fig. 6*C*), AS160^{Ser588} (Fig. 6*D*), Akt^{Thr308} (Fig. 6*F*), or Akt^{Ser473} (Fig. 6*G*) in siPP1-β–transfected cells compared with control cells.

Transfection of L6 cells with siPP1-γ1 caused a substantial and significant ($P < 0.05$) reduction in PP1-γ1 protein abundance compared with cells transfected with the scrambled control siRNA (Fig. 7*A*). The specificity of the PP1-γ1 knockdown was demonstrated by unchanged PP1-α or PP1-β levels (Fig. 7*B*). The lower PP1-γ1 abundance resulted in no changes in the phosphorylation of AS160^{Thr642} (Fig. 7*C*), AS160^{Ser588} (Fig. 7*D*), Akt^{Thr308} (Fig. 7*F*), or Akt^{Ser473} (Fig. 7*G*) in siPP1-γ1–transfected cells versus control cells.

AS160 Dephosphorylation in Muscles From LZ versus OZ Rats

The relative phosphorylation of AS160^{Thr642} was significantly ($P < 0.05$) lower for epitrochlearis muscle lysates from OZ versus LZ rats at 5 min (Fig. 8*A* and *C*). The relative phosphorylation of AS160^{Ser588} was significantly ($P < 0.05$) lower for OZ versus LZ at 30 and 40 min (Fig. 8*B* and *C*). In contrast to AS160 phosphorylation, there were no significant differences between LZ and OZ rats for phosphorylation of Akt^{Thr308} (Fig. 8*D* and *F*) or Akt^{Ser473} (Fig. 8*E* and *F*).

Epitrochlearis muscle lysates from LZ versus OZ did not differ for protein abundance of AS160 (P = 0.42), PP1-α (P = 0.78), or Inh-2 (P = 0.27) (data not shown). Neither did epitrochlearis muscle lysates from LZ versus OZ differ with regard to the amount of AS160-associated PP1-α (P = 0.40) determined by Co-IP (data not shown).

DISCUSSION

Protein phosphorylation status reflects the balance of phosphorylation by kinases and dephosphorylation by phosphatases. However, there is an extreme disparity in

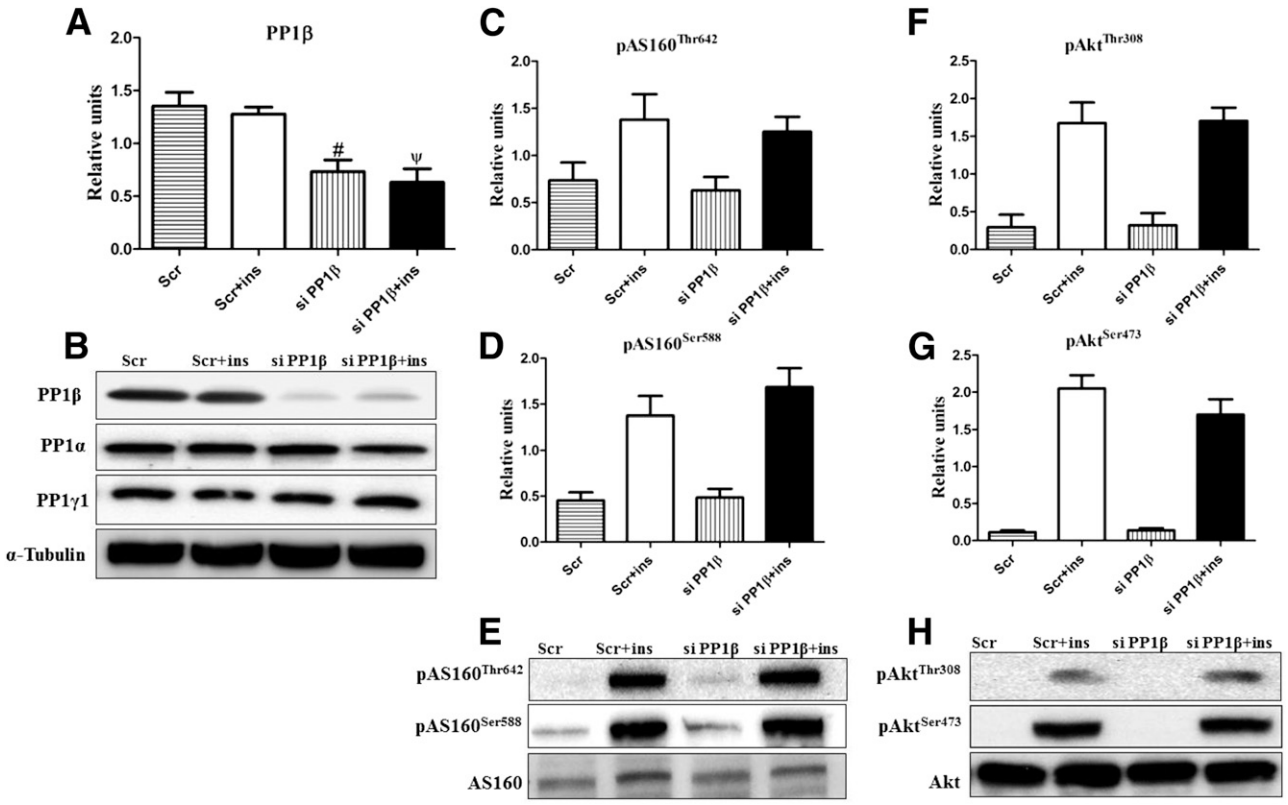

Figure 6—Effects of silencing PP1-β on AS160 phosphorylation in L6 myocytes. L6 cells were transfected with siPP1β or scrambled (Scr) siRNA and treated with insulin (ins) as described for Fig. 5. Protein abundance and phosphorylation were assessed by immunoblotting. PP1-β (A); representative immunoblots of PP1-β, PP1-α, PP1-γ1, and α-tubulin (*B*); pAS160^{Thr642} (*C*); pAS160^{Ser588} (*D*); representative immunoblots of pAS160^{Thr642}, pAS160^{Ser588}, and total AS160 (*E*); pAkt^{Thr308} (*F*); pAkt^{Ser473} (*G*); and representative immunoblots of pAkt^{Thr308}, pAkt^{Ser473}, and total Akt (*H*). Values are expressed as mean ± SEM (n = 4 experiments). Data were analyzed using a two-tailed t test. #$P < 0.05$, siPP1-β is less than Scr for cells incubated without insulin; ψ$P < 0.05$, siPP1-β is less than Scr for cells incubated with insulin.

the level of knowledge about the roles of specific kinases compared with phosphatases in the regulation of protein phosphorylation. Although AS160 phosphorylation is a key determinant of insulin-stimulated glucose transport, prior research had not identified the serine/threonine protein phosphatases that regulate AS160 dephosphorylation. The current study tackled this important problem using a series of different experimental approaches leading to the discovery that PP1-α modulates AS160 dephosphorylation on Ser^{588} and Thr^{642} in skeletal muscle.

PP1, PP2A, PP2B, and PP2C are four of the most highly expressed serine/threonine phosphatases in skeletal muscle (14). We initially tested AS160 dephosphorylation in muscle using several pharmacologic inhibitors that are commonly used to block each of these phosphatases. This first screening step provided no evidence that PP2B or PP2C inhibitors delayed AS160 dephosphorylation on either AS160 phosphorylation site. OA was tested at two doses because it has differing potency for inhibiting PP2A (requiring a lower dose) compared with PP1 (requiring a higher dose) (23). The higher OA dose but not the lower OA dose delayed AS160 dephosphorylation on Thr^{642}. This result is consistent with the possibility that PP1 regulated AS160 dephosphorylation on this site, but a caveat is that this OA dose also produced greater Akt phosphorylation. Both OA doses delayed AS160 dephosphorylation on Ser^{588} concomitant with increased Akt phosphorylation. Earlier research has indicated that OA can attenuate Akt dephosphorylation (24–26). The OA results did not conclusively isolate the possible roles of PP1 or PP2A for controlling AS160 dephosphorylation, so we subsequently used additional experimental approaches to gain more specific insights.

For our first alternative approach, we used Inh-2 to specifically assess the role of PP1 in regulating AS160 dephosphorylation. The results from the rInh-2 experiment were simpler to interpret because Inh-2 selectively inhibits PP1 without inhibiting PP2A (27) and because Inh-2 caused greater phosphorylation on both AS160 sites in the absence of altered Akt phosphorylation. These observations implicated PP1 in the regulation of AS160 dephosphorylation on both Ser^{588} and Thr^{642}. However, because skeletal muscle expresses three PP1 isoforms (PP1-α, PP1-β, and PP1-γ1) and Inh-2 can bind and

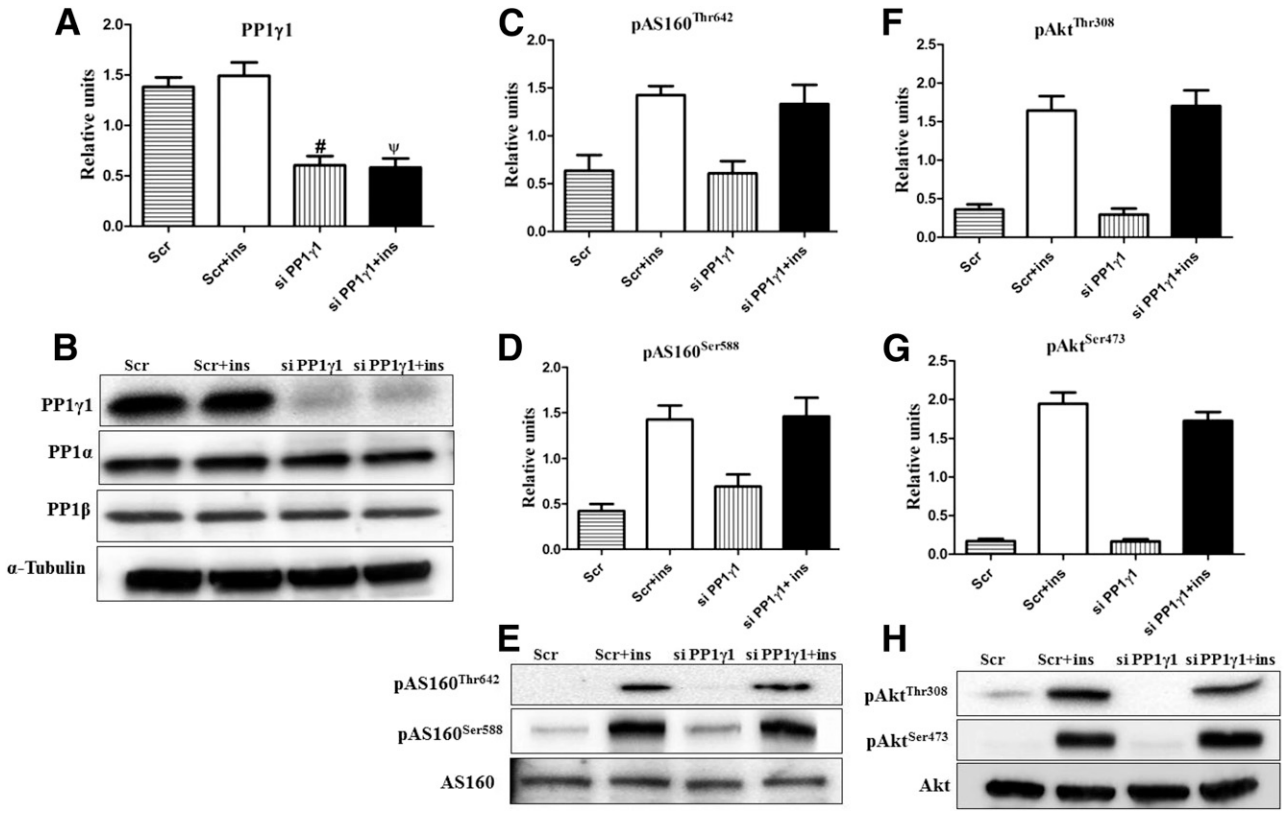

Figure 7—Effects of silencing PP1-γ1 on AS160 phosphorylation in L6 myocytes. Cells were transfected with siPP1-γ1 or scrambled (Scr) siRNA and treated with insulin (ins) as described for Fig. 5. Knockdown was confirmed by measuring the protein abundance of PP1-γ1. Protein abundance and phosphorylation were assessed by immunoblotting. PP1γ1 (*A*); representative immunoblots of PP1-γ1, PP1-α, PP1-β, and α-tubulin (*B*); pAS160^{Thr642} (*C*); pAS160^{Ser588} (*D*); representative immunoblots of pAS160^{Thr642}, pAS160^{Ser588}, and AS160 (*E*); pAkt^{Thr308} (*F*); pAkt^{Ser473} (*G*); and representative immunoblots of pAkt^{Thr308}, pAkt^{Ser473}, and Akt (*H*). Values are expressed as mean ± SEM (n = 4 experiments). Data were analyzed using a two-tailed t test. #$P < 0.05$, siPP1-γ1 is less than Scr for cells treated without insulin; ψ$P < 0.05$, siPP1-γ1 is less than Scr for cells treated with insulin.

inhibit each of these PP1 isoforms (28), it was necessary to next address the possibility of PP1 isoform selectivity.

We used two distinct approaches to address the role of different PP1 isoforms. We first performed Co-IP analysis to evaluate the physical association between AS160 and candidate phosphatases (29). We found that AS160 was selectively associated with PP1-α and not PP1-β or PP1-γ1 in both rat skeletal muscle and L6 myocytes. There was also no evidence for specific interaction between AS160 and PP2A in rat skeletal muscle or L6 cells.

The Co-IP analysis demonstrated that PP1-α and AS160 are binding partners, but this approach cannot establish if there is a functional relationship between the two proteins. Accordingly, we next turned to siRNA silencing to test for PP1 isoform–specific effects. The results of this experiment were invaluable because they clearly revealed that a selective reduction in PP1-α protein abundance produced greater AS160 phosphorylation on Ser^{588} and Thr^{642}. Importantly, Akt phosphorylation was unaltered by PP1-α knockdown, so the greater AS160 phosphorylation was not an indirect consequence of greater Akt phosphorylation. Furthermore, PP1-α knockdown was specific, because there were no changes in the abundance of the other PP1 isoforms. In contrast to the significant effects of PP1-α knockdown, neither PP1-β nor PP1-γ1 knockdown altered AS160 phosphorylation.

It seems possible that altered serine/threonine dephosphorylation of AS160 may contribute to attenuated AS160 phosphorylation that has been reported in insulin-resistant muscles. For example, OZ rats compared with LZ rats are characterized by reductions in insulin-stimulated AS160 phosphorylation and glucose uptake (30–33). The current study included the first evaluation of the potential role of accelerated AS160 dephosphorylation in insulin-resistant muscles. Results from the AS160 dephosphorylation assay revealed modestly faster dephosphorylation of AS160 on Ser^{588} and Thr^{642} in muscle lysates from insulin-resistant OZ rats versus LZ controls. These differences were not explained by disparities in the abundance of AS160, PP1-α, or Inh-2 protein or in the association between PP1-α and AS160. However, these results do not eliminate the possibility of a role for PP1-α in the dysregulation of AS160 phosphorylation in insulin-resistant muscle.

In conclusion, AS160 plays a pivotal role in insulin's regulation of glucose transport in skeletal muscle. Many

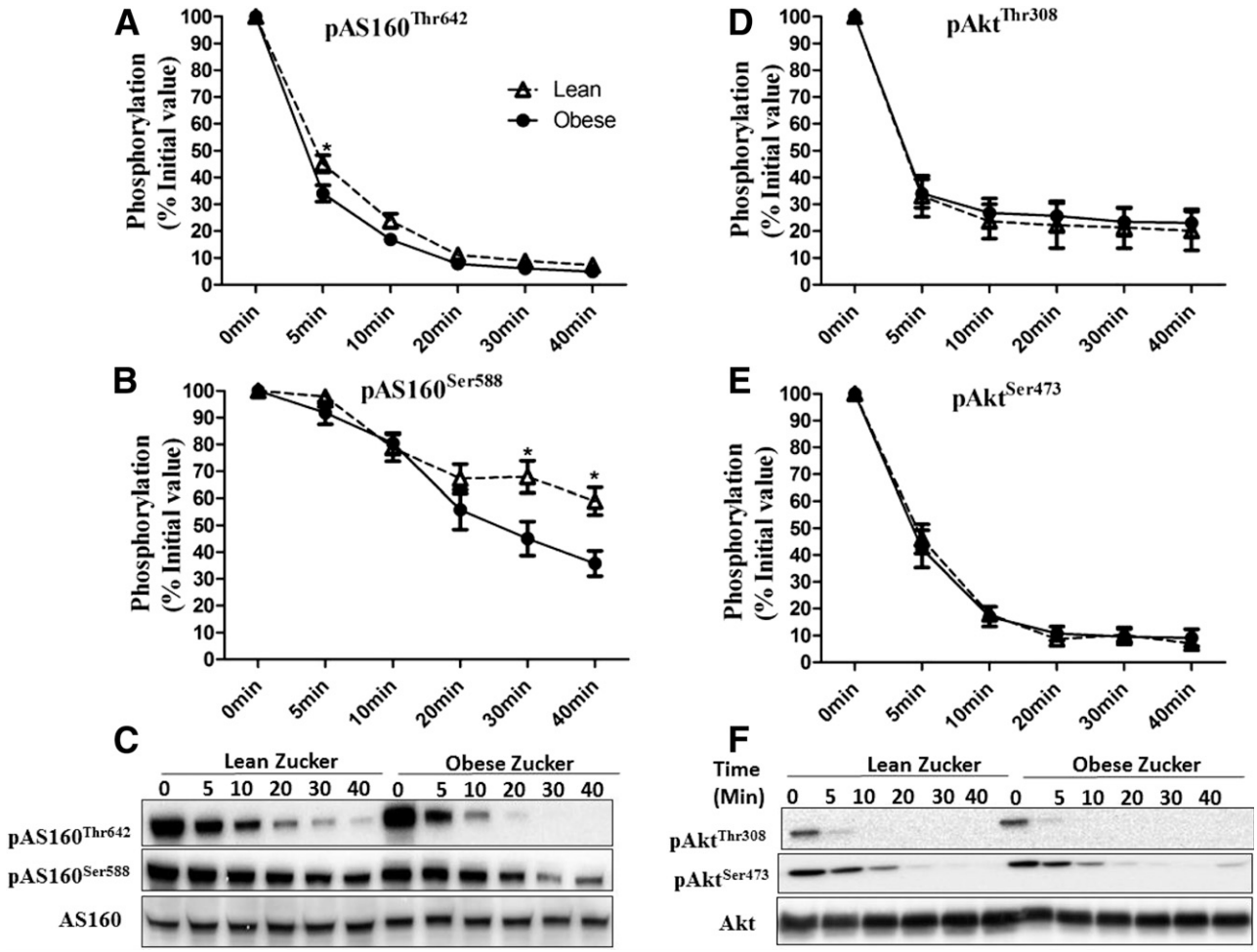

Figure 8—Comparison of AS160 dephosphorylation in epitrochlearis muscle lysates from LZ vs. OZ rats. Isolated muscles from LZ and OZ rats were incubated with insulin (30 nmol/L) for 30 min. The dephosphorylation assay was as described for Fig. 1, except that lysates were incubated at 37°C for 5, 10, 20, 30, and 40 min without the addition of any phosphatase inhibitors. The initial phosphorylation levels for AS160 and Akt were determined for each sample and denoted as 0 min, with a value equal to 100%. The relative phosphorylation values for AS160 and Akt were plotted at each time point: $pAS160^{Thr642}$ (*A*); $pAS160^{Ser588}$ (*B*); representative immunoblots of $pAS160^{Thr642}$, $pAS160^{Ser588}$, and total AS160 (*C*); $pAkt^{Thr308}$ (*D*); $pAkt^{Ser473}$ (*E*); and representative immunoblots of $pAkt^{Thr308}$, $pAkt^{Ser473}$, and total Akt (*F*). Values are expressed as mean ± SEM ($n = 7$ animals for each group). Data were analyzed using a two-tailed *t* test. $^*P < 0.05$ indicates lean exceeds obese at the corresponding times.

previous studies have focused on the role of Akt in the insulin-stimulated phosphorylation of AS160. In contrast, the current study was the first to focus on identifying the serine/threonine phosphatases that control the dephosphorylation of AS160. We discovered that PP1-α regulates AS160 dephosphorylation on Ser^{588} and Thr^{642}, two key sites that control insulin-stimulated glucose transport. This knowledge represents an essential building block for fully understanding the processes that control this key insulin signaling protein that is a crucial regulator of insulin-stimulated glucose transport.

Acknowledgments. The authors acknowledge Naveen Sharma, PhD, currently of Central Michigan University, for his role in the initial development of the dephosphorylation assay.

Funding. This research was supported by a grant from the National Institutes of Health (R01-DK-071771).

Duality of Interest. No potential conflicts of interest relevant to this article were reported.

Author Contributions. P.S. performed the experiments, analyzed the data, designed the experiments, discussed the manuscript, developed the hypothesis, and wrote the manuscript. E.B.A. performed the experiments, analyzed the data, and discussed the manuscript. G.D.C. designed the experiments, coordinated and directed the project, developed the hypothesis, discussed the manuscript, and wrote the manuscript. G.D.C. is the guarantor of this work and, as such, had full access to all the data in the study and takes responsibility for the integrity of the data and the accuracy of the data analysis.

References

1. DeFronzo RA, Jacot E, Jequier E, Maeder E, Wahren J, Felber JP. The effect of insulin on the disposal of intravenous glucose. Results from indirect calorimetry and hepatic and femoral venous catheterization. Diabetes 1981;30:1000–1007

2. Karlsson HK, Zierath JR. Insulin signaling and glucose transport in insulin resistant human skeletal muscle. Cell Biochem Biophys 2007;48:103–113

3. Cartee GD. Roles of TBC1D1 and TBC1D4 in insulin- and exercise-stimulated glucose transport of skeletal muscle. Diabetologia 2015;58:19–30
4. Sakamoto K, Holman GD. Emerging role for AS160/TBC1D4 and TBC1D1 in the regulation of GLUT4 traffic. Am J Physiol Endocrinol Metab 2008;295:E29–E37
5. Cartee GD, Funai K. Exercise and insulin: convergence or divergence at AS160 and TBC1D1? Exerc Sport Sci Rev 2009;37:188–195
6. Sano H, Kane S, Sano E, et al. Insulin-stimulated phosphorylation of a Rab GTPase-activating protein regulates GLUT4 translocation. J Biol Chem 2003;278: 14599–14602
7. Brautigan DL. Protein Ser/Thr phosphatases–the ugly ducklings of cell signalling. FEBS J 2013;280:324–345
8. Shi Y. Serine/threonine phosphatases: mechanism through structure. Cell 2009;139:468–484
9. Gonzalez E, McGraw TE. Insulin-modulated Akt subcellular localization determines Akt isoform-specific signaling. Proc Natl Acad Sci U S A 2009;106: 7004–7009
10. Sharma N, Arias EB, Sequea DA, Cartee GD. Preventing the calorie restriction-induced increase in insulin-stimulated Akt2 phosphorylation eliminates calorie restriction's effect on glucose uptake in skeletal muscle. Biochim Biophys Acta 2012;1822:1735–1740
11. Ng Y, Ramm G, Lopez JA, James DE. Rapid activation of Akt2 is sufficient to stimulate GLUT4 translocation in 3T3-L1 adipocytes. Cell Metab 2008;7:348–356
12. Kramer HF, Witczak CA, Fujii N, et al. Distinct signals regulate AS160 phosphorylation in response to insulin, AICAR, and contraction in mouse skeletal muscle. Diabetes 2006;55:2067–2076
13. Ikubo M, Wada T, Fukui K, et al. Impact of lipid phosphatases SHIP2 and PTEN on the time- and Akt-isoform-specific amelioration of TNF-alpha-induced insulin resistance in 3T3-L1 adipocytes. Am J Physiol Endocrinol Metab 2009; 296:E157–E164
14. Ingebritsen TS, Blair J, Guy P, Witters L, Hardie DG. The protein phosphatases involved in cellular regulation. 3. Fatty acid synthesis, cholesterol synthesis and glycolysis/gluconeogenesis. Eur J Biochem 1983;132:275–281
15. Eto M, Brautigan DL. Endogenous inhibitor proteins that connect Ser/Thr kinases and phosphatases in cell signaling. IUBMB Life 2012;64:732–739
16. Haeseleer F, Sokal I, Gregory FD, Lee A. Protein phosphatase 2A dephosphorylates CaBP4 and regulates CaBP4 function. Invest Ophthalmol Vis Sci 2013; 54:1214–1226
17. Cohen P, Holmes CF, Tsukitani Y. Okadaic acid: a new probe for the study of cellular regulation. Trends Biochem Sci 1990;15:98–102
18. Aburai N, Yoshida M, Ohnishi M, Kimura K. Sanguinarine as a potent and specific inhibitor of protein phosphatase 2C in vitro and induces apoptosis via phosphorylation of p38 in HL60 cells. Biosci Biotechnol Biochem 2010;74:548–552
19. Fruman DA, Bierer BE, Benes JE, Burakoff SJ, Austen KF, Katz HR. The complex of FK506-binding protein 12 and FK506 inhibits calcineurin phosphatase activity and IgE activation-induced cytokine transcripts, but not exocytosis, in mouse mast cells. J Immunol 1995;154:1846–1851
20. Esteves SL, Domingues SC, da Cruz e Silva OA, Fardilha M, da Cruz e Silva EF. Protein phosphatase 1α interacting proteins in the human brain. OMICS 2012;16:3–17
21. Kao SC, Chen CY, Wang SL, et al. Identification of phostensin, a PP1 F-actin cytoskeleton targeting subunit. Biochem Biophys Res Commun 2007;356:594–598
22. Heroes E, Lesage B, Görnemann J, Beullens M, Van Meervelt L, Bollen M. The PP1 binding code: a molecular-lego strategy that governs specificity. FEBS J 2013;280:584–595
23. Bialojan C, Takai A. Inhibitory effect of a marine-sponge toxin, okadaic acid, on protein phosphatases. Specificity and kinetics. Biochem J 1988;256:283–290
24. Thayyullathil F, Chathoth S, Shahin A, et al. Protein phosphatase 1-dependent dephosphorylation of Akt is the prime signaling event in sphingosine-induced apoptosis in Jurkat cells. J Cell Biochem 2011;112:1138–1153
25. Liu W, Akhand AA, Takeda K, et al. Protein phosphatase 2A-linked and -unlinked caspase-dependent pathways for downregulation of Akt kinase triggered by 4-hydroxynonenal. Cell Death Differ 2003;10:772–781
26. Borgatti P, Martelli AM, Tabellini G, Bellacosa A, Capitani S, Neri LM. Threonine 308 phosphorylated form of Akt translocates to the nucleus of PC12 cells under nerve growth factor stimulation and associates with the nuclear matrix protein nucleolin. J Cell Physiol 2003;196:79–88
27. Hurley TD, Yang J, Zhang L, et al. Structural basis for regulation of protein phosphatase 1 by inhibitor-2. J Biol Chem 2007;282:28874–28883
28. Alessi DR, Street AJ, Cohen P, Cohen PT. Inhibitor-2 functions like a chaperone to fold three expressed isoforms of mammalian protein phosphatase-1 into a conformation with the specificity and regulatory properties of the native enzyme. Eur J Biochem 1993;213:1055–1066
29. Virshup DM, Shenolikar S. From promiscuity to precision: protein phosphatases get a makeover. Mol Cell 2009;33:537–545
30. Thyfault JP, Cree MG, Zheng D, et al. Contraction of insulin-resistant muscle normalizes insulin action in association with increased mitochondrial activity and fatty acid catabolism. Am J Physiol Cell Physiol 2007;292:C729–C739
31. Benton CR, Holloway GP, Han XX, et al. Increased levels of peroxisome proliferator-activated receptor gamma, coactivator 1 alpha (PGC-1alpha) improve lipid utilisation, insulin signalling and glucose transport in skeletal muscle of lean and insulin-resistant obese Zucker rats. Diabetologia 2010;53:2008–2019
32. Mackrell JG, Cartee GD. A novel method to measure glucose uptake and myosin heavy chain isoform expression of single fibers from rat skeletal muscle. Diabetes 2012;61:995–1003
33. Etgen GJ Jr, Wilson CM, Jensen J, Cushman SW, Ivy JL. Glucose transport and cell surface GLUT-4 protein in skeletal muscle of the obese Zucker rat. Am J Physiol 1996;271:E294–E301